Journal of Cellular Biochemistry 76:254–269 (1999)

A Novel Human Nucleoside Diphosphate (NDP) Kinase, Nm23-H6, Localizes in Mitochondria and Affects Cytokinesis

Hiromasa Tsuiki,[1,2] Masayuki Nitta,[1,2] Akiko Furuya,[3] Nobuo Hanai,[3] Toshiyoshi Fujiwara,[4] Masaki Inagaki,[5] Masato Kochi,[2] Yukitaka Ushio,[2] Hideyuki Saya,[1] and Hideo Nakamura[1,2]*

[1]Department of Tumor Genetics and Biology, Kumamoto University School of Medicine, Kumamoto 860–0811, Japan
[2]Department of Neurosurgery, Kumamoto University School of Medicine, Kumamoto 860–0811, Japan
[3]Tokyo Research Laboratories, Kyowa Hakko Kogyo Co. Ltd., Machida, Tokyo 194–8533, Japan
[4]First Department of Surgery, Okayama University Medical School, Okayama 700–0914, Japan
[5]Department of Biochemistry, Aichi Cancer Research Institute, 1–1 Kanokoden, Chikusa-ku, Nagoya, Aichi, 464–0021, Japan

Abstract Nucleoside diphosphate kinases (NDP kinases) are enzymes known to be conserved throughout evolution and have been shown to be involved in various biological events, in addition to the "housekeeping" phosphotransferase activity. We present the molecular cloning of a novel human NDP kinase gene, termed *Nm23-H6*. *Nm23-H6* gene has been mapped at chromosome 3p21.3 and is highly expressed in heart, placenta, skeletal muscle, and some of the cancer cell lines. Recombinant Nm23-H6 protein has been identified to exhibit functional NDP kinase activity. Immunolocalization studies showed that both endogenous and inducibly expressed Nm23-H6 proteins were present as short, filament-like, perinuclear radical arrays and that they colocalized with mitochondria. Cell fractionation study also demonstrated the presence of Nm23-H6 protein in a mitochondria-rich fraction. Moreover, induction of overexpression of Nm23-H6 in SAOS2 cells, using the Cre-loxP gene activation system, resulted in growth suppression and generation of multinucleated cells. Flow cytometric analysis also demonstrated that the proportion of cells with more than 4N DNA content increased to 28.1% after induction of Nm23-H6, coinciding with the appearance of multinucleated cells. These observations suggest that Nm23-H6, a new member of the NDP kinase family, resides in mitochondria and plays a role in regulation of cell growth and cell cycle progression. J. Cell. Biochem. 76:254–269, 1999.

Key words: NDP kinase; mitochondria; multinucleated cells; Cre-mediated gene activation system; 3p21.3

Nucleoside diphosphate kinases (NDP kinases) are enzymes that are conserved throughout evolution and ubiquitously expressed. The NDP kinases play a major role in the synthesis of nucleoside triphosphates by catalyzing the transfer of the γ-phosphate of 5′-triphosphate nucleotides to 5′-diphosphate nucleotides. In addition to their "housekeeping" phosphotransferase activity, NDP kinases expressed in mammalian cells are involved in various biological events such as tumor metastasis, cell proliferation, differentiation, motility, transcriptional regulation, development, senescence, and apoptosis [Biggs et al., 1990; de la Rosa et al., 1995; Kantor et al., 1993; Keim et al., 1992; Nosaka et al., 1998; Okabe et al., 1988; Postel et al., 1993; Venturelli et al., 1995].

The gene *Nm23-M1*, which encodes an active NDP kinase, was originally identified by its reduced expression in highly metastatic K-1735 murine melanoma cell lines, as compared to low metastatic melanoma cell lines [Steeg et al., 1988]. In humans, several NDP kinases have been identified [Milon et al., 1997; Munier et al., 1998; Rosengard et al., 1989; Stahl et al., 1991; Venturelli et al., 1995]. *Nm23-H1*, the human homologue of *Nm23-M1*, has been reported as a tumor metastasis suppressor gene and transfection of *Nm23-H1* cDNA into hu-

*Correspondence to: Hideo Nakamura, Department of Tumor Genetics and Biology, Kumamoto University School of Medicine, 2–2-1 Honjo, Kumamoto 860–0811, Japan.

Received 24 March 1999; Accepted 10 July 1999

man breast cancer cell lines resulted in inhibition of metastatic potential and malignant progression in vivo. Nm23-H2 has been reported to function as a transcriptional regulatory factor, Puf, for the c-*myc* proto-oncogene promoter [Postel et al., 1993]. DR-nm23, which was identified by differential screening of a complementary DNA (cDNA) library derived from chronic myelogenous leukemia cells in blast crisis, inhibits granulocyte colony-stimulating factor (G-CSF)-stimulated granulocytic differentiation and induces apoptosis when overexpressed in myeloid precursor cells [Venturelli et al., 1995]. Interestingly, some of these functions, such as metastatic potential, transcriptional regulation, and inhibition of differentiation, do not require NDP kinase activity [MacDonald et al., 1993; Okabe et al., 1995: Postel and Ferrone, 1994], suggesting that NDP kinases play roles in a wide variety of cellular events, not only as enzymes but also as signaling molecules.

We present the molecular cloning and characterization of a novel human NDP kinase gene, termed *Nm23-H6*. Immunolocalization studies demonstrated that Nm23-H6 protein was detected mainly in mitochondria. Moreover, the induction of Nm23-H6 overexpression in SAOS2 cells using the Cre-loxP gene activation system resulted in growth suppression and the generation of multinucleated cells. These observations suggested that Nm23-H6, a mitochondria-localizing, novel, human NDP kinase, may play a role in cell growth and cell cycle progression.

MATERIALS AND METHODS

Cell Lines

The following cell lines were maintained in RPMI 1640 medium supplemented with 10% heat-inactivated fetal calf serum (FCS), 100 U/ml penicillin, and 100 U/ml streptomycin sulfate (Gibco-BRL, Rockville, MD): COS7, an SV40-transformed monkey kidney cell; EJ, a human bladder carcinoma; H1299, a human lung large cell carcinoma; T98G and U251MG, human astrocytomas; HeLa S3, a human uterine cervical cell carcinoma; VA13, an SV40-transformed human lung fibroblast; U2OS and SAOS2, human osteosarcomas; HL-60, a human promyelocytic leukemia; K563, a human chronic myelogenous leukemia; Raji, Burkitt's lymphoma; SW480, KM12C and KM12SM human colorectal adenocarcinomas; SN12C and SN12PM6, human renal cell carcinomas.

Adenovirus Vectors

Replication-deficient recombinant adenovirus vectors described previously [Kanegae et al., 1995; Miyake et al., 1998] were used in this study; Ad5CMV-p53 expressed human wild-type p53 driven by the human cytomegalovirus (CMV) early promoter. Ad5CMV-Luc expressing luciferase was used as the control vector. Cre-recombinase expressing adenovirus, AxCANCre, was provided by Dr. Saitoh (University of Tokyo). Adenoviruses were propagated in the 293-transformed human embryonic kidney cell line that readily permits the replication of these E1 replication-deficient adenoviruses. The viral titration was performed using a plaque assay described previously [Miyake et al., 1998].

Cloning of the cDNA for Functional Complementation of the p53-Induced Apoptosis

An SAOS2 osteosarcoma cell line was cotransfected with plasmids pSVneo and pCMV-EBNA by liposome-mediated gene transfer method and subsequently selected with 400 μg/ml G418 (Gibco-BRL). The clonal line showing the highest transfection efficiency with plasmid pDR2 was designated SAOS2-EBNA and used for further experiments.

To screen for complementation of SAOS2-EBNA cells with a HeLa cell cDNA library in a pDR2 EBV-based vector, 7.5×10^4 SAOS2-EBNA cells/ml in serum free RPMI 1640 were transfected with 200 μg of the HeLa cDNA library by the liposome-mediated gene transfer method. At 5 days post-transfection, SAOS2-EBNA cells were infected with Ad5CMV-p53 expressing human wild-type p53 protein (100 pfu/cell) in RPMI 1640 medium supplemented with 10% FCS. At 7 days after the adenoviral infection, surviving cells were collected. The episomal plasmids were rescued by alkaline lysis and transformed into *Escherichia coli*, DH5α. The cDNA insert of the rescued plasmid was sequenced by the dideoxychain termination method on 373 sequencer (PE Applied Biosystems, Foster City, CA), using pDR2 vector sequencing primers (pDR2 sense primer (5′-CTGGTAAGTTTAGTCTTTTTGTC-3′) and pDR2-antisense primer (5′-GTGCCA AGCTTG-CATGCCTG-3′)). DNA and protein sequences were compared using the basic local alignment search tool (BLAST) from the National Center for Biotechnology Information (NCBI).

Northern Blot Analysis

Northern blots from multiple human tissues and cancer cell lines containing 2 μg of poly $(A)^+$ RNA per lane were obtained from Clontech (Palo Alto, CA). The membranes were probed with a full-length cDNA fragment of *Nm23-H6* that had been labeled with [α-^{32}P]dCTP by random-primer labeling. The membranes were exposed to X-ray film with an intensifying screen for 3 days at −70°C.

PCR Mapping of *Nm23-H6* Gene

Radiation hybrid mapping of the *Nm23-H6* gene was performed as previously described [Makino et al., 1997] using a set of primers (S-1: 5′-CAAGCCTGATGCA GGTCTATGAAG-3′ and AS-1: 5′-AAGAAGTAGATAGAAGGCTAGATC-3′) whose design was based on the partial genomic sequence of the *Nm23-H6* gene. The S-1 and AS-1 primers were expected to amplify a 198-base pair (bp) polymerase chain reaction (PCR) product from human genomic DNA as a template. The PCR results of the Radiation Hybrid Panel were sent to the Whitehead Institute/MIT Center for Genome Research via WWW (http://www-genome.wi.mit.edu/) for mapping of the genes relative to the radiation hybrid map of the human genome [Hudson et al., 1995].

Purification of GST Fusion Protein

Human recombinant Nm23-H6 were produced as fusion proteins with 26-kDa glutathione S-transferase (GST) in *E. coli* and purified as follows. The full length of *Nm23-H6* cDNA was amplified by PCR from the pDR2/p53R-1 plasmid using r*Tth* DNA polymerase (PE Applied Biosystems) and a set of primers: S-*Bam*HI (5′-TGGGGGGATCCATGACCCAGA-ATCTGGGGAGTGA-3′) containing a *Bam*HI site (underlined) and AS-*Hin*dIII (5′-GAAGG-TACCTCAGGCTGGTCCTAGGCC TCC-3′) containing a *Hin*dIII site. The PCR fragments were digested with *Bam*HI and *Hin*dIII, and ligated inframe to a pGEX-2TH expression vector. The pGEX-2T-Nm23-H1 plasmid was provided by Dr. Furukawa (Nagoya University). A culture of *E. coli* DH5α transformed with each plasmid was diluted 1:10 in 1,000 ml of fresh LB medium containing ampicillin (50 μg/ml) and incubated for 26 h. After 6 h of growth, isopropyl-1-thio-β-D-galactopyranoside (TAKARA, Shiga, Japan) was added to a final concentration of 0.1 mM. Bacterial cultures were centrifuged, and the resulting pellet was resuspended in 50 ml buffer. The cells were lysed on ice by gentle sonication and centrifuged at 20,000*g* for 20 min at 4°C. The supernatant was mixed at 4°C in a polypropylene tube on a rotating platform with 5 ml glutathione-Sepharose beads that had been previously washed and resuspended in phosphate-buffered saline (PBS). After absorption for 2 h, the beads were collected and eluted with elution buffer (50 mM Tris, pH 9.5, 10 mM glutathione). After dialysis with a sufficient amount of PBS, the quality and quantity of purified proteins were confirmed by Coomassie brilliant blue staining and by Western blotting.

In Vitro Autophosphorylation and NDP Kinase Assay

For autophosphorylation, 15 μg of purified proteins conjugated with 15 μg glutathione agarose beads was incubated in 30 μl of reaction buffer containing 20 mM Tris, pH 7.5, 100 mM NaCl, 10 mM $MgCl_2$, 1 mM dithiothreitol, 10 mM cold ATP, and 2 μCi of [γ-^{32}P]ATP at 30°C for 20 min. After washing the beads three times with washing buffer (20 mM Tris, 100 mM NaCl, 1 mM dithiothreitol) to remove free [γ-^{32}P]ATP, reaction beads were diluted with SDS sample loading buffer. The phosphorylated proteins were separated by sodium dodecyl sulfate-polyacrylamide gel electrophoresis (SDS-PAGE) and visualized by autoradiography.

NDP kinase activity of the GST-fusion protein was determined by thin-layer chromatography (TLC). For the assay, 15 μg of purified proteins conjugated with 15 μg glutathione agarose beads was incubated in 30 μl of reaction buffer prescribed for autophosphorylation assay. After the beads were washed with washing buffer, they were incubated with 30 μl of second reaction buffer containing 20 mM Tris, pH 7.5, 100 mM NaCl, 10 mM $MgCl_2$, 1 mM dithiothreitol, 1 mM cold CDP as the γ-phosphate acceptor at 30°C for 20 min. Aliquots from each reaction were spotted onto a PEI-cellulose-F TLC plate (Merck, Darmstadt, Germany). The spotting sample volume of GST-Nm23-H1 was 30 times less than the others. This ratio was calculated with NIH image software regarding the result of autophosphorylation assay. The synthesis of [γ-^{32}P]CTP was analyzed by ascending chromatography with 0.75 M KH_2PO_4, pH

3.6. The TLC plate was air-dried, and the nucleotides were visualized by autoradiography.

Production of Anti-Nm23-H6 Monoclonal Antibody

Balb/c mice were immunized 3 times at 2-week intervals by intraperitoneal injection of a synthetic peptide (CYSPEGGVHYVAGTGGL-GPA) that was coupled to KLH. The mice were sacrificed 3 days after the final immunization, and spleen cells were fused with mouse myeloma P3-U1 cells as described previously [Saya et al., 1986]. Culture supernatants from wells showing active cell growth were tested for reactivity to the peptide. A monoclonal antibody that specifically recognizes Nm23-H6 was selected and purified by column chromatography with protein A-Sepharose.

Construction of the Nm23-H6 Expression Plasmid

The full-length open reading frame (ORF) of the *Nm23-H6* cDNA (585-bp) was amplified by PCR from the pDR2/p53R-1 plasmid, using r*Tth* DNA polymerase and a set of primers: S-*Eco*RI (5′-TGGGGGAATTCATGACCCAGAATCTG-GG GAGTGA-3′) containing an *Eco*RI site (underlined) and AS-*Kpn*I (5′-GAAGGTACC TCAG-GCTGG TCCTAGGCCTCC-3′) containing a *Kpn*I site (underlined). The PCR fragments were digested with *Eco*RI and *Kpn*I and ligated into a pBj-Myc expression vector.

Western Blotting

For Western blot analysis, samples containing equal amounts of protein (10 µg) from lysates of cultured cells and from recombinant GST fusion protein were separated on a 12% or 15% polyacrylamide gel and transferred to a nitrocellulose filter with a constant current of 140 mA for 1.5 h. The filters were blocked overnight at 4°C with PBS containing 10% skim milk, incubated with 1:1,000 diluted anti-GST antibody (MBL, Nagoya, Japan), 1:500 diluted anti-Nm23-H6 antibody, mAb-KM2102, 1:500 diluted anti-3-oxoacyl-CoA thiolase antibody in PBS containing 0.03% Tween 20 for 1 h, and washed three times for 5 min each time with PBS containing 0.3% Tween 20. The filters were then incubated with horseradish peroxidase (HRP)-conjugated anti-mouse IgG antibody for the first antibody for 1 h and then washed three times for 7 min each time with PBS containing 0.3% Tween 20. Specific proteins were detected using enhanced chemiluminescence (ECL) (Amersham, Buckinghamshire, England).

Cell Fractionation

Cell fractionation was performed using the method described previously [Yano et al., 1997]. Briefly, 1×10^6 U2OS cells were washed twice with PBS and harvested by trypsinization. The pellet was suspended in 150 µl of ice-cold PBS. The cell suspensions were treated with equal volumes of 0.5 mg/ml digitonin in PBS for 2 min on ice. The homogenate was centrifuged at 15,000*g* for 2 min. This supernatant was designated the soluble cytosol fraction, which scarcely contained mitochondria. Subsequently, the pellet was suspended with 300 µl of 0.5% TritonX-100 in PBS and centrifuged at 15,000*g* for 2 min. This supernatant was designated as the mitochondria-rich fraction and the final pellet designated the insoluble cytoskeletal fraction. Each fraction was diluted with SDS sample loading buffer and assayed by Western blot as described above.

Immunofluorescence Procedure and Confocal Laser Scanning Microscopic Analysis

Immunofluorescence microscopic analysis was performed as previously described [Koga et al., 1998]. U2OS cells and SAOS2 cells grown on Labtek chamber slides (Nunc, Naperville, IL) were fixed in 4% paraformaldehyde for 10 min, followed by 0.2% Triton X-100 for 5 min. For mitochondria staining, living cells were incubated with Mitotracker Red CMX-ROS (100 nM, 30 min, Molecular Probes, Eugene, OR) before fixation. After washing with PBS, sample cells were incubated with 1:50 diluted anti-Nm23-H6 antibody, mAb-KM2102, 1:10,000, diluted rat anti-tubulin antibody (Harlan Sera-Lab, Loughborough, England), 1:100 diluted γ-tubulin antibody (Sigma Chemical Co., St. Louis, MO) for 1 h. After another wash with PBS, the cells were incubated with species-appropriate fluorescein-conjugated secondary antibodies. For nuclear staining, propidium iodide was used after 10-min RNase treatment. After washing with PBS, the cells were mounted in 80% glycerol and visualized with a confocal microscope (Fluoview, Olympus, Tokyo, Japan) equipped with an argon gas laser and appropriate filter sets to permit recording of fluorescein. Throughout this study, we confirmed that no

bleed-through occurred between different channels by comparing the results obtained by depleting one primary antibody.

Inducible Expression of the Nm23-H6 in SAOS2 Cells

The constructs corresponding to the Cre-mediated Nm23-H6 expression plasmid were generated by ligating the *Eco*RI/*Kpn*I fragment containing the full-length ORF of the *Nm23-H6* cDNA into a pCALNL5 plasmid which has a Cre-mediated activation unit [Kanegae et al., 1995, 1996]. These constructs were named pCALNL5-Nm23-H6. The plasmids were transfected into SAOS2 cells by the liposome-mediated gene transfer method. Clones were selected in a medium containing 400 μg/ml G418 (Gibco-BRL). The drug-resistant cell lines were infected with AxCANCre adenovirus, which produces Cre recombinase for 12 h, and then the medium was changed to adenovirus-free growing medium. The infected cells were then prepared for further experiments.

Growth Curve

Cells (5×10^4) were seeded in 6-well plates and allowed to attach overnight. The next day, the medium was replaced with fresh culture medium containing Ad5CMV-Luc or AxCANCre. According to the experimental time course, these cells were trypsinized and harvested, and the total number of the cells were counted and calculated. Each assay was preformed in triplicate.

Flow Cytometric Analysis

Cells were harvested using trypsin and washed with PBS and then fixed in 70% methanol in PBS for 1 h at 4°C. They were then stained with propidium iodide (50 ng/ml in PBS) containing 0.2 mg/ml RNase A, and the DNA content was measured using a flow cytometer (FACScan, Becton Dickinson, MountainView, CA) to analyze the cell cycle.

RESULTS

Identification of a Novel Nucleoside Diphosphate Kinase, Nm23-H6

An 1166-bp cDNA that encoded a sequence containing a long open reading frame (ORF) was discovered fortuitously in a screen for genes that suppressed p53-induced apoptosis in the SAOS2 osteosarcoma cell line. In our experiments, reintroduction of this cDNA expression plasmid into SAOS2 cell has not effectively prevented induction of apoptosis due to adenovirus-mediated *p53* gene transfer. However, since the protein encoded by this cDNA was novel and shared high homology with the Nm23 protein family, we attempted to characterize this gene, termed *Nm23-H6*. The predicted amino acid sequence of the *Nm23-H6* gene showed high similarity to sea urchin dynein intermediate chain 1 and the nucleoside diphosphate kinases of various species (Fig. 1). The overall amino acid sequence of Nm23-H6 has 40% identity with sea urchin dynein intermediate chain 1, 40% identity with *E. coli* NDP kinase, 37% identity with DR-nm23, 33% identity with Nm23-H2, 31% identity with Nm23-H4, and 31% identity with Nm23-H1.

It has been proposed that NDP kinase activity depends on the formation of a transient, high-energy phosphorylation intermediate form of the enzyme due to phosphorylation of a histidine residue. The probable histidine phosphorylation site is conserved at residue 137 (H137) of Nm23-H6. Furthermore, all the key residues (Lys27, Tyr68, Phe76, Arg104, Thr110, Arg124, Asn134, and Glu148), which are conserved in all other NDP kinases and involved in nucleotide binding and catalysis based on the crystallographic [Webb et al., 1995] and biological studies [Freije et al., 1997], are also found in Nm23-H6.

Expression and Chromosomal Localization of *Nm23-H6* Gene

To determine the expression pattern of *Nm23-H6* mRNA, we performed Northern blot analysis on various human tissues and cell lines. *Nm23-H6* transcripts approximately 2 kb in size were detected higher levels in the heart, placenta and skeletal muscles. *Nm23-H6* transcripts were also expressed in various cell lines and the expression levels differed among cell lines (Fig. 2).

To identify the chromosomal localization of the *Nm23-H6* gene, we performed PCR-based radiation hybrid mapping using primers designed on the basis of a partial genomic DNA sequences of the *Nm23-H6* gene. PCR products of the expected sizes (198 bp) were amplified from 26 of 93 hybrid cell lines in the Genebridge

```
              Nm23-H6     1 MTQNLGSEMASILRS P------QALQLTLA LIKPDAVAHPLILEA VHQQILSNKFLIVRM RELLWRKEDCQRFYR 69
intermediate chain 1    177 VSQGTVDTLMHG-RQ DGPQTEPVPKEVTVV LIKPDAVANGHVDSI IAK-IEEHGFEILTT EDKTLTEDEAREFYK 250
          NDPK/E.coli     1 ---------------- -------MAIERTFS IIKPNAVAKNVIGNI FAR-FEAAGFKIVGT KMLHLTVEQARGFYA 52
              DR-nm23     1 MICLVLTIFANLFPA ACTGA----HERTFL AVKPDGVQRRLVGEI VRR-FERKGFKLVAL KLVQSSEELLREHYA 70
              Nm23-H2     1 --------MANL--- ----------ERTFI AIKPDGVQRGLVGEI IKR-FEQKGFRLVAM KFLRASEEHLKQHYI 53
              Nm23-H4    13 LRCGPRAPGPSLLVR HGSGGPSWTRERTLV AVKPDGVQRRLVGDV IQR-FERRGFTLVGM KMLQAPESVLAEHYQ 86
              Nm23-H1     1 --------MANC--- ----------ERTFI AIKPDGVQRGLVGEI IKR-FEQKGFRLVGL KFMQASEDLLKEHYV 53
                                                          K                                   Y

              Nm23-H6    70 EHEGRFFYQRLVEFM ASGPIRAYILA---- HKDAIQLWRTLMGPT RVFRARHVAPDSIRG SFGLTDTRNTTHGSD 140
intermediate chain 1   251 QHEEEEHFEVLVTFM ASGPSKILVLTRGDT GEGVVSEVRNLLGPK DIEVAKEEAPDSLRA QFGTDKKMNAMHGAD 325
          NDPK/E.coli    53 EHDGKPFFDGLVEFM TSGPIVVSVLE---- GENAVQRHRDLLGAT NPANA---LAGTLRA DYADSLTENGTHGSD 120
              DR-nm23    71 ELRERPFYGRLVKYM ASGPVVAMVWQ---- GLDVVRTSRALIGAT NPADA---PPGTIRG DFCIEVG-NLIHGSD 138
              Nm23-H2    54 DLKDRPFFPGLVKYM NSGPVVAMVWE---- GLNVVKTGRVMLGET NPADS---KPGTIRG DFCIQVGRNIIHGSD 121
              Nm23-H4    87 DLRRKPFYPALIRYM SSGPVVAMVWE---- GYNVVRASRAMIGHT DSAEA---APGTIRG DFSVHISRNVIHASD 154
              Nm23-H1    54 DLKDRPFFAGLVKYM HSGPVVAMVWE---- GLNVVKTGRVMLGET NPADS---KPGTIRG DFCIQVGRNIIHGSD 121
                                 F                                 R     T            R         N  *

              Nm23-H6   141 SVVSASREIAAFFPD FSEQRWYEEEEPQLR CGPVCYSPEGGVHYV AGTGGLGPA 194
intermediate chain 1   326 SKETAAREMAFLLPN FSVPIVPGTGPPPTI EKTLALIRPSALKDH KDEMLQKIQ 379
          NDPK/E.coli   121 SVESAAREIA----- ----YFFGEGE---- ---VCPRTR------ --------- 143
              DR-nm23   139 SVESARREIA----- ----LWFRADE---- ---LLCWEDSAGHWL YE------- 168
              Nm23-H2   122 SVKSAEKEIS----- ----LWFKPEE---- ---LVDYKSCAHDWV YE------- 152
              Nm23-H4   155 SVEGAQREIQ----- ----LWFQSSE---- ---LVSWADGGQHSS IHPA----- 187
              Nm23-H1   122 SVESAEKEIG----- ----LWFHPEE---- ---LVDYTSCAQNWI YE------- 152
                                   E
```

Fig. 1. Deduced amino acid sequence of the *Nm23-H6* gene and comparison of sequence identities in Nm23-H6, to sea urchin dynein intermediate chain 1, *Escherichia coli* NDP kinase and various human NDP kinases. The protein sequences were compared using the Multiple Sequence Alignments at BCM Search Launcher (http://dot.imgen.bcm.tmc.edu:9331/multi-align/multi-align.html). Amino acid residues identical to Nm23-H6 protein in the same position are shaded. The asterisk under Nm23-H1 indicates the probable histidine phosphorylation site. The key residues conserved in all NDP kinase homologues are written beneath in bold. The cDNA sequence has been submitted to the GenBank database (accession no. U90449).

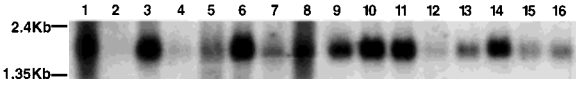

Fig. 2. Northern blot analysis of *Nm23-H6*. Each lane contained 2 µg of human poly(A)$^+$ RNA. Human tissues from heart (**lane 1**), brain (**lane 2**), placenta (**lane 3**), lung (**lane 4**), liver (**lane 5**), skeletal muscle (**lane 6**), kidney (**lane 7**), and pancreas (**lane 8**); and cell lines HL-60 (**lane 9**), HeLa S3 (**lane 10**), K562 (**lane 11**), Molt4 (**lane 12**), Raji (**lane 13**), SW480 (**lane 14**), A549 (**lane 15**), and CT361 (**lane 16**). Blots were hybridized with a specific cDNA probe for *Nm23-H6*. The size marker (kb) is indicated.

4 radiation hybrid panel. Comparison with the human chromosomal content of the hybrids, as determined by the producer and the Whitehead Institute/MIT Center for Genome Research, localized the *Nm23-H6* gene to chromosome 3p21.3 and placed it 4.29 cR from AFMB362WB9 (Fig. 3).

Nm23-H6 Is a Novel Member of the Human NDP Kinases

Since the deduced amino acid sequences of Nm23-H6 are similar to the NDP kinase of various species, we examined whether Nm23-H6 has a NDP kinase activity. Phosphorylation of NDP by NDP kinase is thought to occur in two steps:

Step 1: N_1TP + NDP kinase ↔ N_1DP + NDP kinase-His-P

Step 2: N_2DP + NDP kinase-His- P ↔ N_2TP + NDP kinase

At first, we examined autophosphorylation (step 1) of purified GST-Nm23-H6. As shown in Figure 4A, GST-Nm23-H6 was detected as a phosphorylated band, but phosphorylation activity was about 30 times less than that of Nm23-H1.

Subsequently, we examined the activity of the phosphorylated enzyme intermediate to phosphorylate NDP to NTP. Although autophosphorylation of Nm23-H6 was much less than Nm23-H1, it was possible that essential NDP kinase activity of Nm23-H6 might have been similar to that of Nm23-H1. The autophosphorylated GST-Nm23-H6 fusion protein was able to transfer [γ-^{32}P]phosphate from [γ-^{32}P]ATP to CDP and produced the [γ-^{32}P]CTP; the GST protein did not exhibit catalytic activity (Fig. 4B). The activity of the phosphorylated enzyme intermediate of GST-Nm23-H6 was almost the

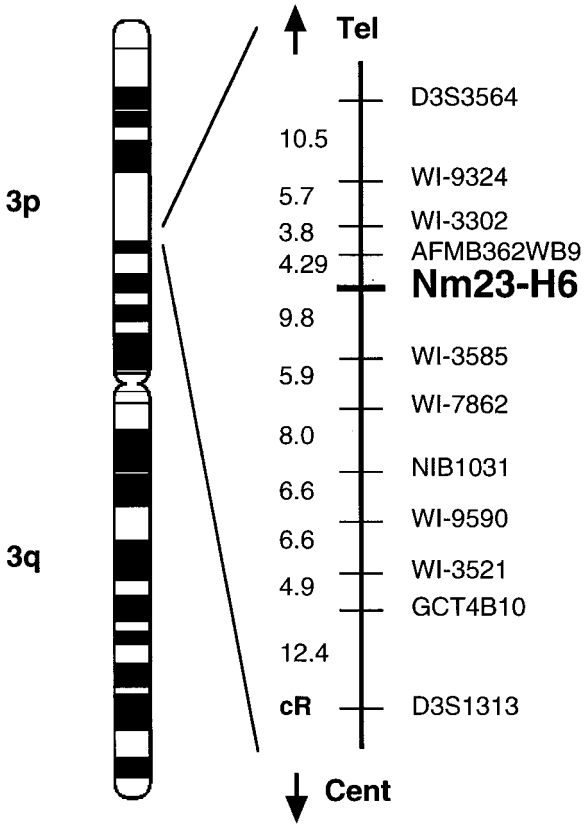

Fig. 3. Chromosomal localization of the *Nm23-H6* gene by radiation hybrid mapping. The results of PCR using the radiation hybrid panel were sent to the Whitehead Institute/MIT Center for Genome Research via WWW. The *Nm23-H6* gene was placed at 4.29 cR from AFMB362WB9 microsatellite marker on chromosome 3p21.3.

same as GST-Nm23-H1. These findings demonstrate that Nm23-H6 is a novel member of human NDP kinases.

Expression and Subcellular Localization of Nm23-H6 Protein

To examine the expression of Nm23-H6 protein, we developed a monoclonal antibody, termed mAb-KM2102, against the Nm23-H6 by immunizing a mouse with a synthetic peptide derived from the amino acid sequence of Nm23-H6. The mAb-KM2102 could detect a specific band of 24 kDa in the lysate from COS-7 cells that were transiently transfected by pBj-Myc-Nm23-H6 (Fig. 5A). This antibody also specifically recognized the recombinant GST-Nm23-H6 protein, but not GST-Nm23-H1 and GST (Fig. 5B). Using this antibody, the expression of endogenous Nm23-H6 protein in several cell lines was examined by Western blotting. Although

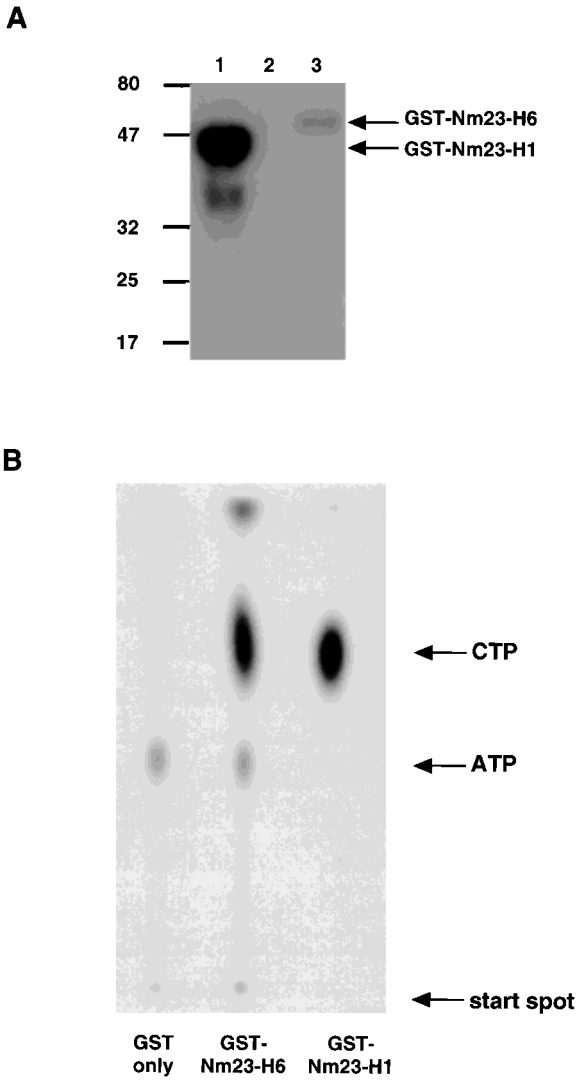

Fig. 4. **A:** Autophosphorylation activity of recombinant Nm23-H6 protein. Purified GST fusion proteins (**lane 1**, GST-Nm23-H1; **lane 2**, GST only; **lane 3**, GST-Nm23-H6) immobilized on glutathione agarose beads were incubated with [γ-^{32}P]ATP. After washing to remove free [γ-^{32}P]ATP, the beads were diluted with SDS sample loading buffer. The phosphorylated proteins were separated by sodium dodecyl sulfate-polyacrylamide gel lectrophoresis (SDS-PAGE) and visualize by autoradiography. The positions of autophosphorylated GST fusion proteins are indicated on the right. **B:** NDP kinase activity of recombinant Nm23-H6 protein. Purified GST fusion proteins (**lane 1**, GST only; **lane 2**, GST-Nm23-H6; **lane 3**, GST-Nm23-H1) immobilized on glutathione agarose beads were incubated with [γ-^{32}P]ATP. After washing, the beads were incubated with cold CDP, and the formation of [γ-^{32}P]CTP was analyzed by thin-layer chromatography and autoradiography. The position of residual [γ-^{32}P]ATP and produced [γ-^{32}P]CTP are indicated on the right.

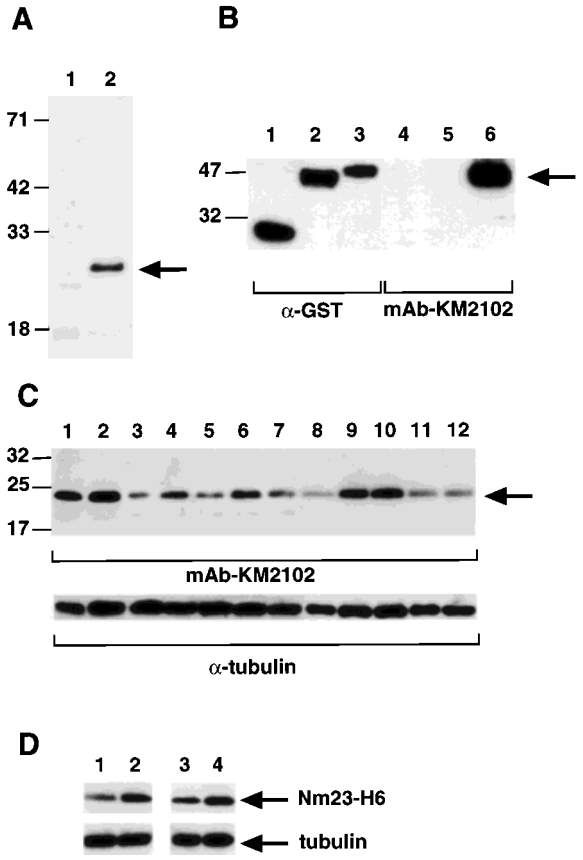

Fig. 5. Western blot analysis of Nm23-H6 using Nm23-H6 specific monoclonal antibody, mAb-KM2102. **A:** Lysates prepared from COS-7 cells (**lane 1**) and pBj-Myc-Nm23-H6 transfected COS-7 cells (**lane 2**) were detected by mAb-KM2102. **B:** Recombinant GST (**lanes 1, 4**), GST-Nm23-H1 (**lanes 2, 5**) and GST-Nm23-H6 (**lanes 3, 6**) were detected by anti-GST antibody (**lanes 1, 2, 3**) and by mAb-KM2102 (**lanes 4, 5, 6**). Arrow, the 50-kDa GST-Nm23-H6 protein. **C:** Lysates prepared from various cell lines (EJ, H1299, T98G, U251MG, VA13, U2OS, SAOS2, HL-60, HeLa S3, K562, Raji, and SW480: **lanes 1–12**) were detected by mAb-KM2102. Arrow, the 22-kDa endogenous Nm23-H6 protein. **D:** Lysates prepared from SN12C (low metastatic clone: **lane 1**), SN12PM6 (high metastatic clone: **lane 2**), KM12C (low metastatic clone: **lane 3**) and KM12SM (high metastatic clone: **lane 4**) were detected by mAb-KM2102 (top) and anti-tubulin (bottom).

there were differences in the expression levels, all cell lines examined expressed a 22-kDa protein, which was specifically recognized by the mAb-KM2102 antibody (Fig. 5C). The molecular mass of 22 kDa is close to the calculated molecular weight of the full-length protein encoded by the *Nm23-H6* cDNA. The EJ, H1299, U251MG, U2OS, HeLaS3, and K562 cell lines were found to express Nm23-H6 protein at high levels, whereas the T98G, VA13, SAOS2, HL-60, and Raji cell lines expressed it at low levels. Five cell lines (HL-60, HelaS3, K562, Raji, and SW480) were analyzed for Nm23-H6 mRNA and protein expression by Northern blot (Fig. 2) and Western blot (Fig. 5C), respectively. The expression level of the mRNA was well correlated with that of the protein in most of the cell lines.

Marked reduction of Nm23-H1 expression has been reported to correlate with metastatic potential of some cancers [de la Rosa et al., 1995]. To examine whether Nm23-H6 level is also involved in metastatic propencity, we investigated the expression of Nm23-H6 protein in SN12C, SN12PM6, KM12C, and KM12SM cells, those are known to have different metastatic potentials [Radinsky et al., 1992] (Fig. 5D). However, Nm23-H6 protein was expressed in all cell lines, regardless of their metastatic potential, and SN12PM6 and KM12SM cells, which have higher metastatic potential, showed higher expression of Nm23-H6 protein than that of low metastatic clones, SN12C and KM12C. These findings suggest that Nm23-H6 may not play a role in suppression of metastatic potential of these human cancer cells.

To examine the subcellular localization of Nm23-H6 protein, we performed immunocytochemical analysis of U2OS cells. The U2OS cells manifested higher expression of Nm23-H6 protein in Western blot analysis (Fig. 5C). Using the mAb-KM2102 antibody, endogenous Nm23-H6 was detected mainly in the cytoplasm; it was stained densely around the nucleus in interphase U2OS cells (Fig. 6A). Short, fragmented, filament-like, perinuclear radical arrays were also observed at the rim of fluorescent signals. Although the association of NDP kinases with microtubules has been previously reported, this subcellular distribution of the Nm23-H6 protein implies that it is associated with mitochondria (Fig. 6B,C).

To further examine the colocalization of Nm23-H6 and mitochondria, we double-labeled U2OS cells with mAb-KM2102 and the rhodamine-based chemical probe MitoTracker, which specifically recognizes mitochondria. In interphase cells, the comparison of the mitochondria-associated rhodamine fluorescence and FITC fluorescence patterns from Nm23-H6 demonstrated that they were essentially identical (Fig. 6D,E), whereas the Nm23-H6 staining was distinct from that of microtubules (Fig. 6F). Moreover, in mitotic phase cells, Nm23-H6 staining

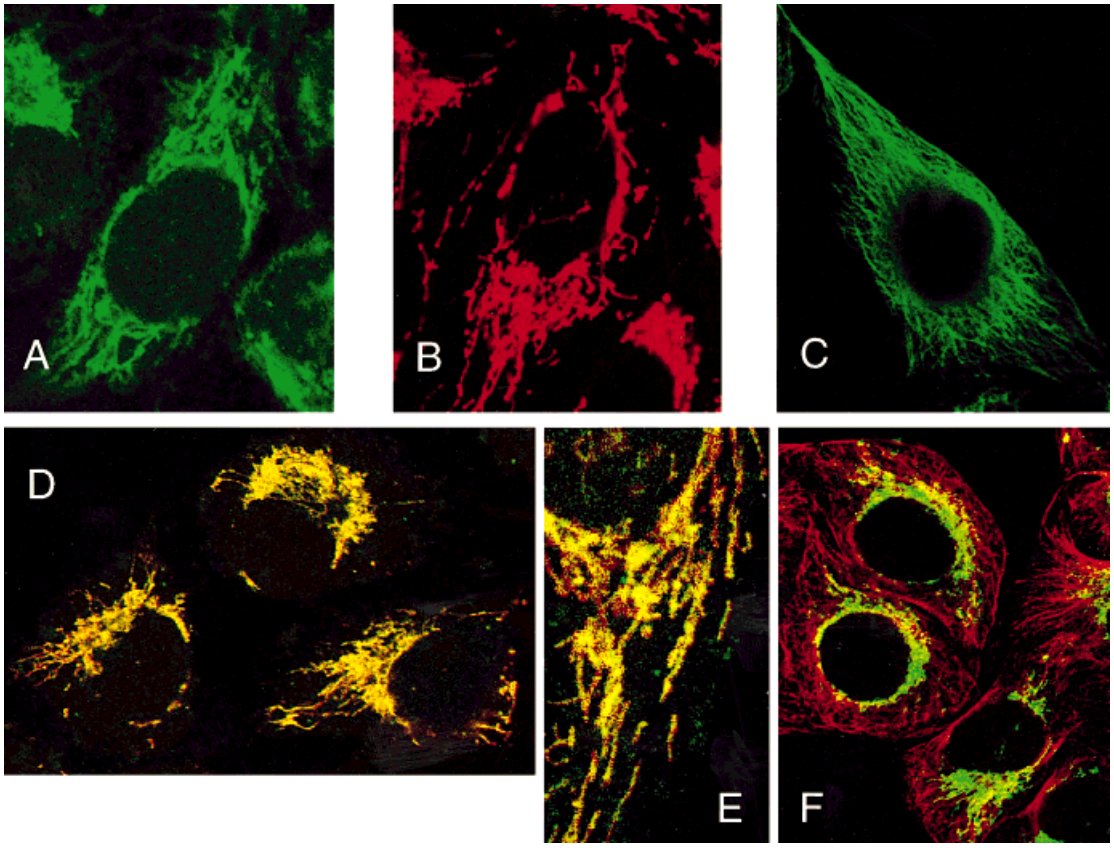

Fig. 6. Immunocytochemical analysis of U2OS cells. **A–C:** U2OS cells in interphase were stained with anti-Nm23-H6 antibody, mAb-KM2102 (A), Mitotracker Red CMX-ROS (B), and anti-tubulin antibody (C). Endogenous Nm23-H6 was observed as short fragmental perinuclear radical arrays in U2OS cells. **D–F:** U2OS cells in interphase were double-labeled with mAb-KM2102 (D–F, green) and Mitotracker CMX-ROS (D, E red) and anti-tubulin antibody (F, red). E: High-resolution photo of a double-labeled U2OS cell with mAb-KM2102 and Mitotracker CMX-ROS.

did not coincide with the mitotic spindle but assumed a cage-like pattern around the outside of both the chromosome and mitotic spindle (data not shown). Staining patterns of Nm23-H6 in the mitotic phase were also similar to the distribution of mitochondria (data not shown). These findings suggest that Nm23-H6 colocalizes with mitochondria rather than with microtubules. Furthermore, the cells were fractionated by digitonin into soluble, mitochondrial, insoluble fractions, and the presence of Nm23-H6 protein in these fractions was detected by Western blot analysis. Nm23-H6 was predominantly detected in the mitochondria-rich fraction that contains a mitochondria-specific enzyme, 3-oxoacyl-CoA thiolase (Fig. 7). All these findings indicate that Nm23-H6 is associated with mitochondria morphologically and biochemically.

Overexpression of Nm23-H6 Causes Cell Growth Suppression and Multinucleated Cells

To understand the biological role of Nm23-H6, we employed inducible overexpression of Nm23-H6 in SAOS2 cells, using the Cre-mediated gene activation system [Kanegae et al., 1995, 1996]. SAOS2 cells, which exhibited low expression of Nm23-H6 protein upon Western blot analysis (Fig. 5B), were transfected with pCALNL5-Nm23-H6, and clones were selected with G418. Cells carrying pCALNL5-Nm23-H6 were grown for 48 h in the presence or absence of the Cre recombinase-producing recombinant adenovirus (AxCANCre).

Western blot analysis revealed that overexpression of Nm23-H6 was induced in the SAOS2-Nm23-H6 cells at 48 h after adenovirus infection (Fig. 8A). When Nm23-H6 expression was induced for more than 72 h, a large number

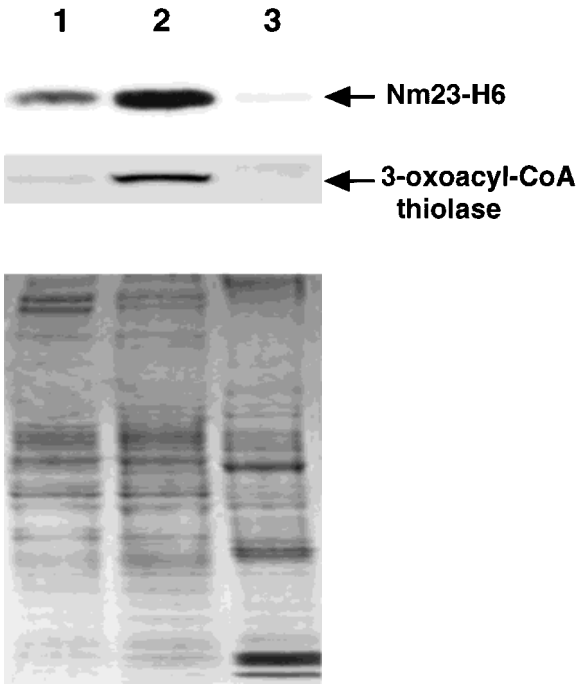

Fig. 7. Western blot analysis of fractionated proteins from U2OS cells, using monoclonal antibody against Nm23-H6, mAb-KM2102. Soluble cytosol fraction (**lane 1**), mitochondrial fraction (**lane 2**), and insoluble cytoskeletal fraction (**lane 3**) were detected by mAb-KM2102 (**top**). The same samples were detected by polyclonal antibody against 3-oxoacyl-CoA thiolase, which specifically exist in mitochondria matrix [Amaya et al., 1988] (**middle**). Equal quantity of proteins was confirmed by Coomassie brilliant blue staining (**bottom**).

of cells became round and tended to detach from the substratum. The growth rate of the AxCANCre-treated SAOS2-Nm23-H6 cells was slower than untreated and Ad5CMV-Luc control adenovirus-treated SAOS2-Nm23-H6 cells (Fig. 8B). By contrast, the growth rate of SAOS2 parent cells remained unchanged even in the absence of treatment, or after AxCANCre and Ad5CMV-Luc control adenovirus treatment. This result indicates that the overexpression of Nm23-H6 protein induces a growth reduction.

Upon immunocytochemical analysis, inducibly expressed Nm23-H6 exhibited a short, fragmented, filamental staining pattern in SAOS2-Nm23-H6 cells. This staining pattern was consistent with that of endogenous Nm23-H6. Nm-23-H6 overexpressed cells frequently became multinucleate, as revealed by an increase in number of nuclei in a cell (Fig. 8C). Staining with an antibody against the centrosome-specific γ-tubulin showed that these cells contained many centrosomes (Fig. 8D). These observations reflected that these abnormally shaped multinucleated cells were generated by a failure of mitosis. At 96 h after the treatment with AxCANCre, 20.4% of SAOS2-Nm23-H6 cells became multinucleate (Fig. 8E). By contrast, AxCANCre-treated SAOS2 cells and Ad5CMV-Luc-treated SAOS2-Nm23-H6 cells mostly exhibited normal morphology. AxCANCre-treated SAOS2-Nm23-H6 cells contained about 5 times more multinuclear cells than did AxCANCre-treated SAOS2 cells or Ad5CMV-Luc-treated SAOS2-Nm23-H6 cells. Although a little more parental SAOS2 cells infected with AxCANCre became multinucleated cells than those infected with Ad5CMV-Luc, there was no statistical significance. However, we cannot completely rule out the possibility that the overexpression of Cre recombinase by adenovirus may have some effects on cell cycle regulation.

The effects of the expression of Nm23-H6 on the cell cycle were also evaluated by flow cytometric analysis (Fig. 9). When overexpression of the Nm23-H6 protein was induced for 96 h, cell populations with 2N DNA significantly decreased and those with 4N DNA content increased. By contrast, AxCANCre treated SAOS2 parent cells and Ad5CMV-Luc adenovirus-treated SAOS2-Nm23-H6 cells displayed normal cell cycle division patterns. In particular, the proportion of cells with more than 4N DNA content increased to 28.1% after induction of Nm23-H6, coinciding with the appearance of multinucleated cells that had more than four nuclei. These observations suggest that overexpression of the Nm23-H6 protein affected the mitotic process, resulting in the generation of multinucleated cells.

DISCUSSION

During the course of screening molecules that suppressed p53-induced apoptosis, we found a gene that encoded a novel NDP kinase, termed *Nm23-H6*. The predicted amino acid sequence of Nm23-H6 showed that all the key residues of the NDP kinase family, previously shown to be crucial for nucleotide binding and catalysis by crystallographic [Webb et al., 1995] and biological studies [Freije et al., 1997], are conserved in Nm23-H6 protein. The probable histidine phosphorylation site for catalysis is especially well conserved at residue 137 (H137) and the NDP kinase consensus motif (NXXHGSD) is completely conserved in Nm23-H6.

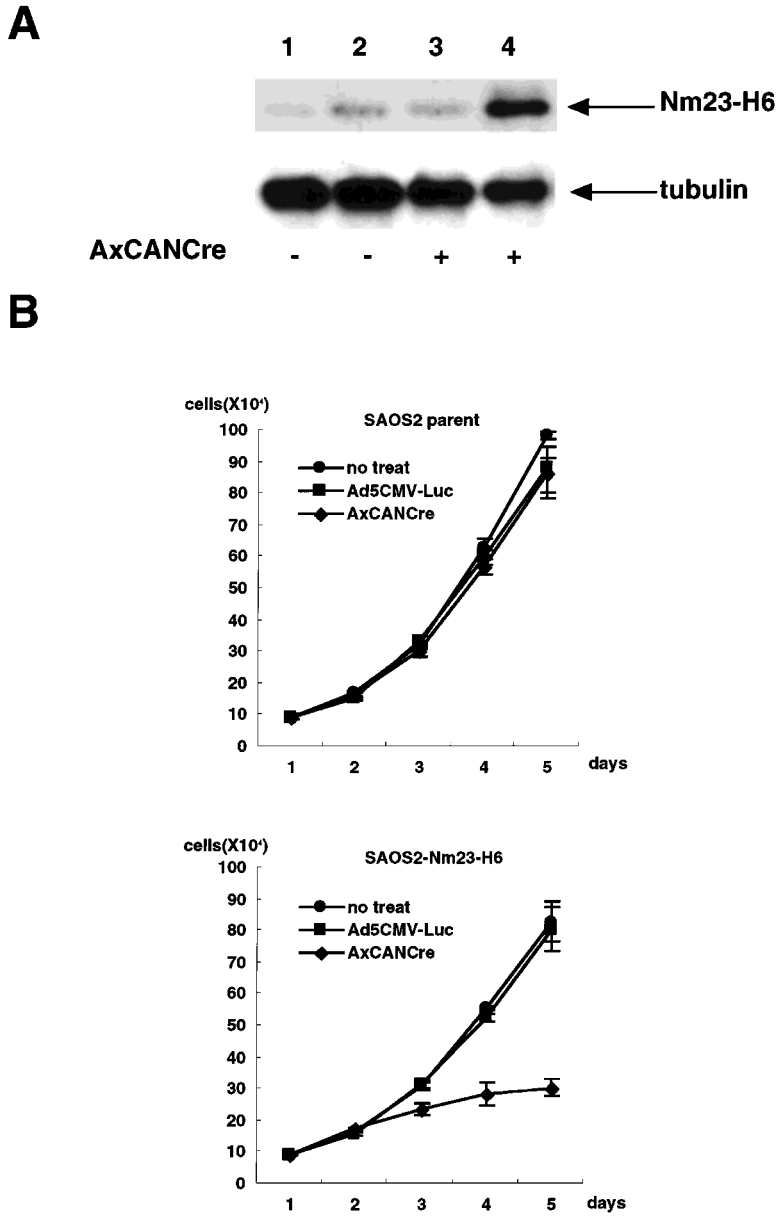

Fig. 8. Cre-mediated Nm23-H6 overexpression in SAOS2 cells. **A:** AxCANCre-induced expression of Nm23-H6 protein in SAOS2 cells was determined by Western blot analysis. Parental SAOS2 cells (**lanes 1, 3**) and SAOS2-Nm23-H6 cells (**lanes 2, 4**) infected (**lanes 3, 4**) or not infected (**lanes 1, 2**) with AxCANCre, the Cre recombinase expression adenovirus. Note the weak endogenous Nm23-H6 protein of the same size in parent SAOS2 cells and SAOS2-Nm23-H6 cells without AxCANCre treatment. **B:** Effect of Cre-mediated Nm23-H6 overexpression in SAOS2 on cell growth. 5×10^4 cells of each cell line were plated on 6-well culture plates and then treated with AxCANCre, Ad5CMV-Luc, or additional culture medium at various time courses. The growth curve was determined by direct cell count. Results are the mean of three independent experiments. Bars = SD. **C:** Immunocytochemical analysis of overexpressed Nm23-H6 protein in SAOS2. Inducibly expressing Nm23-H6 proteins were detected by mAb-KM2102 followed by FITC-conjugated secondary antibody (green fluorescence, right). The nuclei were stained with propidium iodide (red fluorescence, left). A composite image in the center is indicated. **D:** Immunocytochemical analysis of overexpressed Nm23-H6 protein in SAOS2. Centrosome was detected by γ-tubulin followed by FITC-conjugated secondary antibody (green fluorescence, arrow). Nuclei were stained with propidium iodide (red fluorescence). **E:** Induction of multinucleated cells by overexpression of Nm23-H6. The parental SAOS2 cells (columns 1 and 3) and SAOS2-Nm23-H6 cells (columns 2 and 4) were infected with Ad5CMV-Luc control adenovirus (columns 1 and 2) or AxCANCre, the Cre recombinase expression adenovirus (columns 3 and 4). At 96 h after infection, multinucleated cells that had more than four nuclei were counted. The results are the mean of five independent experiments. Bars = SD.

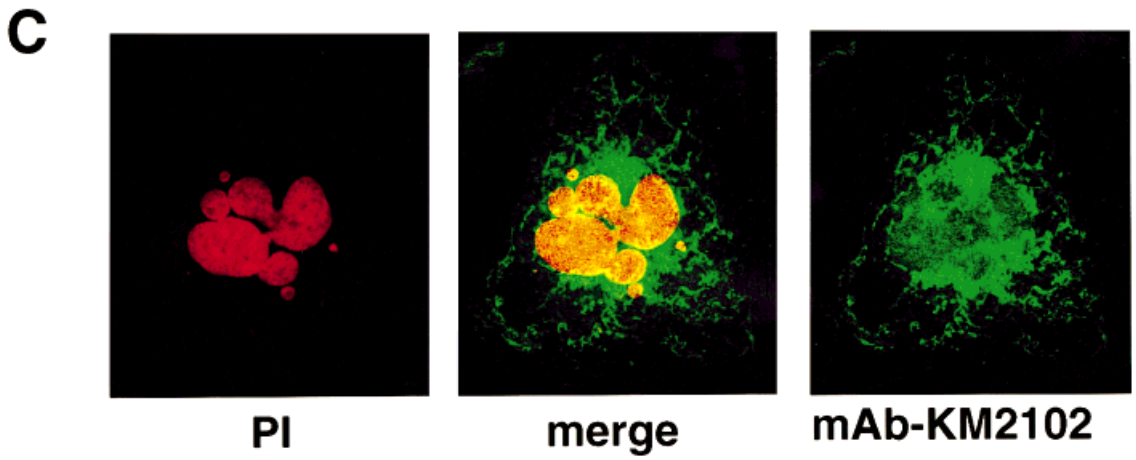

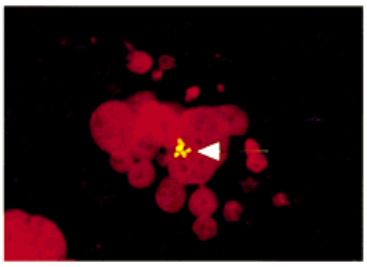

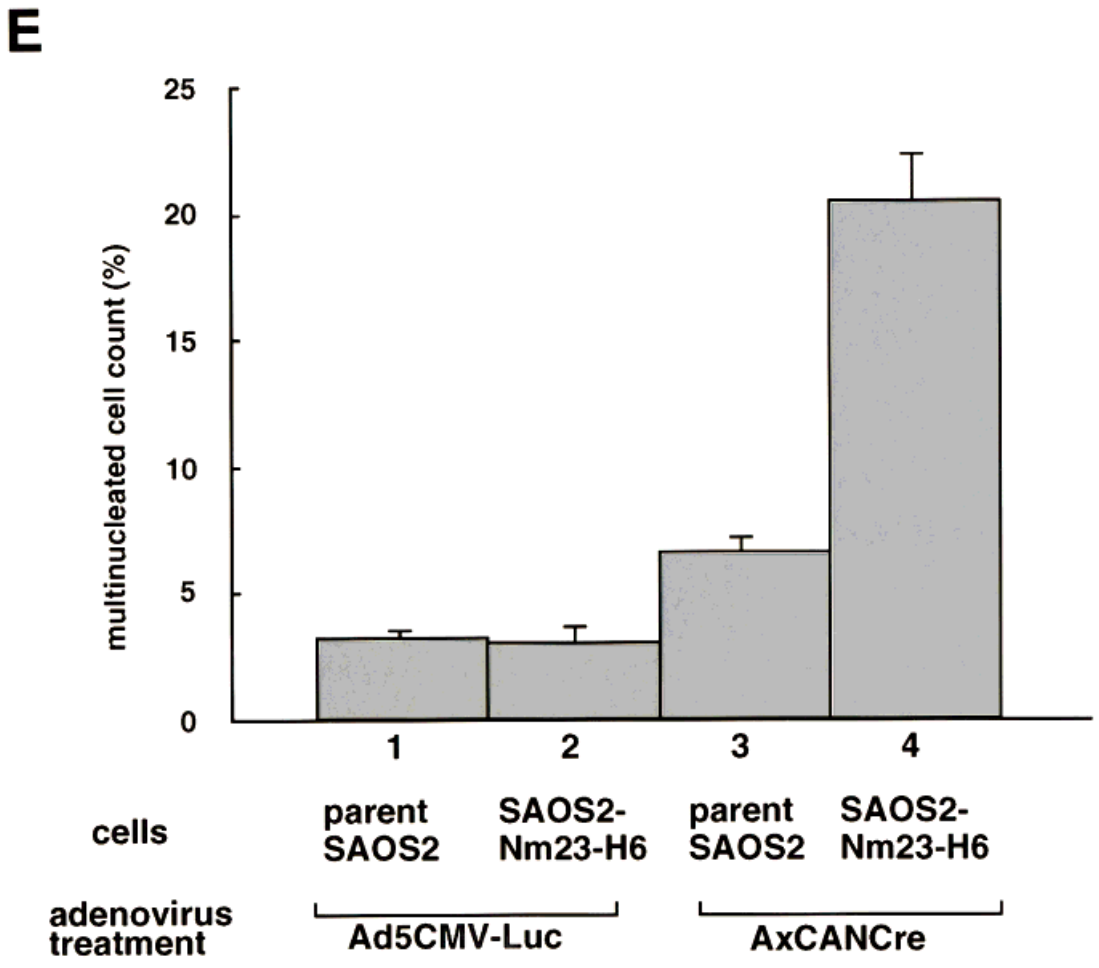

Figure 8. (Continued.)

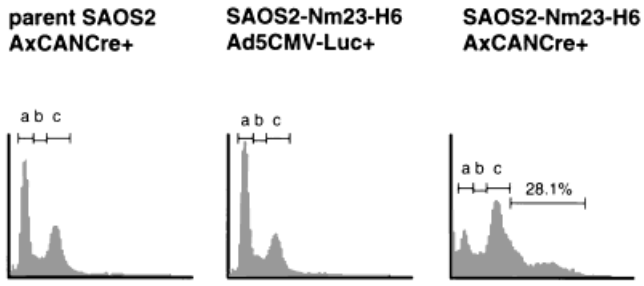

a: G1 (%)	43.1	47.7	15.5
b: S (%)	13.4	14.3	10.5
c: G2-M (%)	33.8	28.9	40.3
G1/G2 ratio	1.28	1.65	0.38

Fig. 9. Cell cycle analysis of SAOS2-Nm23-H6 cells. The parental SAOS2 cells or SAOS2-Nm23-H6 cells were treated with AxCANCre or control Ad5CMV-Luc adenovirus. The cells were harvested at 96 h after the adenovirus treatment, and cell cycle analysis was performed. DNA content, measured by propidium iodide staining, is expressed on the x-axis versus the cell number on the y-axis. Numbers under each histogram represent the percentage of G1, S, G2-M phase cells, and G1/G2 ratios.

NDP kinase is defined as a protein with the ability to transfer γ-phosphate from any nucleoside triphosphate to any other nucleoside diphosphate by a ping-pong mechanism involving a high-energy phosphorylated enzyme intermediate. This pathway is thought to be composed of two sequential reactions: (1) the autophosphorylation of a histidine residue, and (2) phosphotransfer reaction from the phosphohistidine intermediate to NDP [de la Rosa et al., 1995; Freije et al., 1997]. While the autophosphorylation activity of Nm23-H6 is much lower than that of Nm23-H1 under the condition we tested, the phosphotransfer activity of the phosphorylated enzyme intermediate remains functional. The low autophosphorylation activity may be due to the absence of an ATP-binding motif in the Nm23-H6. The predicted amino acid sequence of Nm23-H6 was highly similar to sea urchin dynein intermediate chain 1. Intermediate chain 1, one component of the outer arm dynein of sea urchin sperm axoneme, is a multifunctional protein with an NDP kinase-related region in its middle portion [Ogawa et al., 1996]. However, previous reports revealed that the intermediate chain 1 alone does not exhibit detectable NDP kinase activity, probably because of a lack of the ATP-binding motif [Ogawa et al., 1996]. The dynein intermediate chain 1 interacts with a β-dynein heavy chain that contains four copies of a putative ATP-binding site. Thus, NDP kinase activity of dynein intermediate chain 1 may be activated by forming a complex with other components, such as a β-dynein heavy chain. Moreover, Nm23-H1 was found to form a specific complex with glycelaldehyde-3-phosphate dehydrogenase (GAPDH), which has an ATP binding motif [Engel et al., 1998], and this complex formation resulted in enhancement of NDP kinase activity of Nm23-H1. Similar to the dynein intermediate chain 1 and Nm23-H1, Nm23-H6 may require some interactive protein(s) which promotes phosphorylation of the histidine residue for generating a phosphohistidine intermediate that has sufficient NDP kinase activity. Furthermore, NDP kinase activity may not be essential for the function of Nm23-H6, since both a transcriptional regulatory function and a differentiation inhibitory function of Nm23-H2 were shown to be independent of their NDP kinase activities [Okabe et al., 1995; Postel and Ferrone, 1994].

Our mapping results established that *Nm23-H6* was located on 3p21.3. It is worth noting that frequent chromosome 3p abnormalities and allele loss have been reported in lung and breast cancers [Sekido et al., 1998]. A high incidence of loss of heterozygosity in 3p21 has been reported as one of the early changes in uterine cervical cell transformation [Wistuba et al., 1997]. There is evidence for a nasopharyngeal carcinoma tumor suppressor gene that maps at 3p21.3 between D3S1298 and D3S1578, the region containing the *Nm23-H6* locus [Cheng et al., 1998]. It has been also reported that 3p deletion occurs more frequently in lung tumor tissues from smoking than from nonsmoking patients. Fluorescent in situ hybridiza-

tion (FISH) showed that benzopyrene diol epoxide-induced chromosome 3p21.3 aberrations were significantly more frequent among lung cancer patients who smoked than in control patients [Wu et al., 1998]. These findings suggested the presence of some tumor suppressor genes in the 3p21.3 region. To determine the involvement of the *Nm23-H6* gene in the development of human cancers, further experiments are needed to identify alterations, including deletions and mutations, of the *Nm23-H6* gene.

Our immunocytochemical and biochemical analyses demonstrate that Nm23-H6 protein is associated with mitochondria. The existence of mitochondrial NDP kinase activity was reported as early as 1955 [Herbert et al., 1955], and mitochondrial NDP kinases have been reported in *Dictyostelium discoideum* and pigeon [Lambeth et al., 1997; Troll et al., 1993]. It has been speculated that human Nm23-H4 exists in mitochondria, because it possesses the characteristics of mitochondrial sequences [Milon et al., 1997], but this has not been experimentally confirmed. Therefore, Nm23-H6 is the first human NDP kinase immunocytochemically and biochemically proven to localize in mitochondria.

Overexpression of the Nm23-H6 protein in a Cre-loxP-inducible system induced a growth suppression and markedly increased numbers of multinucleated cells with DNA content over 4N. One way that cells can become polyploid is through the disruption of the mitotic spindle. It has been previously shown that null mutation in the *awd* gene, which encodes the only NDP kinase identified in *Drosophila melanogaster* and is highly homologous to the human Nm23 family, leads to chromosomal condensation and mitotic defects due to disruption of mitotic spindle microtubule polymerization [Biggs et al., 1990]. Several reports suggest a colocalization and biochemical interaction between NDP kinases and microtubules [Biggs et al., 1990; Lombardi et al., 1995; Nickerson and Wells, 1984]. However, our immunolocalization and cell fractionation studies demonstrated that Nm23-H6 resides in mitochondria. Therefore, the multinucleated cells induced by expression of Nm23-H6 may not be directly attributable to mitotic spindle disassembly.

Recent observations have demonstrated that polyploid and/or multinucleated cells are generated not only by disruption of the mitotic spindle but by the inappropriate expression of antiapoptosis genes and the failure of checkpoint controls during cell cycle as well [Bunz et al., 1998; Minn et al., 1996; Taylor and McKeon, 1997]. In particular, cells expressing Bcl-xL, an antiapoptotic protein found in mitochondria, have been reported to show an increased propensity to become polyploid by overcoming a cell cycle checkpoint [Minn et al., 1996]. Similarly, inappropriate expression of Nm23-H6 may induce an imbalance of nucleotide pools in mitochondria, resulting in a failure of checkpoint controls and accumulation of karyotypic abnormalities. It will be important to determine whether NDP kinase activity of Nm23-H6 and proper control of its expression are required for cell cycle regulation and faithful cell division.

ACKNOWLEDGMENTS

We thank Dr. J. Sasaki, Dr. Y. Honda, Dr. N. Mugita, and Dr. M. Nakao (Department of Tumor Genetics and Biology, Kumamoto University) for technical assistance and discussion; Dr. A. Kikuchi (Department of Biochemistry, Hiroshima University), Dr. H. Maruta (Ludwig Institute for Cancer Research), and Dr. K. Furukawa (Department of Biochemistry, Nagoya University) for providing the pBj-Myc, pGEX-2TH, and pGEX-2T-Nm23-H1 plasmids, respectively; Dr. I. Saitoh and Dr.Y. Kanegae (Laboratory of Molecular Genetics, Institute of Medical Science, the University of Tokyo) for providing the Cre-loxP gene activation system; Dr. M. Mori (Institute for Medical Genetics, Kumamoto University) for providing anti-3-oxoacyl-CoA thiolase antibody; Dr. M. Nakajima (Oncology Research, Novartis Pharma) and Dr. K. Gohji (Department of Urology, Osaka Medical Collage) for providing cancer cell lines that have different metastatic potentials; Dr. J. Moon for editing the manuscript; and T. Arino for secretarial assistance. This work was supported by a grant for cancer research from the Ministry of Education, Science and Culture of Japan (to H.S.).

REFERENCES

Amaya Y, Arakawa H, Takiguchi M, Ebina Y, Yokota S, Mori M. 1988. A noncleavable signal for mitochondrial import of 3-oxoacyl-CoA thiolase. J Biol Chem 263:14463–14470.

Biggs J, Hersperger E, Steeg PS, Liotta LA, Shearn A. 1990. A *Drosophila* gene that is homologous to a mammalian gene associated with tumor metastasis codes for a nucleoside diphosphate kinase. Cell 63:933–940.

Bunz F, Dutriaux A, Lengauer C, Waldman T, Zhou S, Brown JP, Sedivy JM, Kinzler KW, Vogelstein B. 1998. Requirement for p53 and p21 to sustain G2 arrest after DNA damage. Science 282:1497–1501.

Cheng Y, Poulos NE, Lung ML, Hampton G, Ou B, Lerman MI, Stanbridge EJ. 1998. Functional evidence for a nasopharyngeal carcinoma tumor suppressor gene that maps at chromosome 3p21.3. Proc Natl Acad Sci USA 95:3042–3047.

de la Rosa A, Williams RL, Steeg PS. 1995. Nm23/nucleoside diphosphate kinase: toward a structural and biochemical understanding of its biological functions. BioEssays 17:53–62.

Engel M, Seifert M, Theisinger B, Seyfert U, Welter C. 1998. Glyceraldehyde-3-phosphate dehydrogenase and Nm23-H1/nucleoside diphosphate kinase A. Two old enzymes combine for the novel Nm23 protein phosphotransferase function. J Biol Chem 273:20058–20065.

Freije JM, Blay P, MacDonald NJ, Manrow RE, Steeg PS. 1997. Site-directed mutation of Nm23-H1. Mutations lacking motility suppressive capacity upon transfection are deficient in histidine-dependent protein phosphotransferase pathways in vitro. J Biol Chem 272:5525–5532.

Herbert E, Potter VR, Takagi Y. 1955. Nucleotide metabolism. IV. The phosphorylation of 5′-uridine nucleotides by cell fractions from rat liver. J Biol Chem 213:923–940.

Hudson TJ, Stein LD, Gerety SS, Ma J, Castle AB, Silva J, Slonim DK, Baptista R, Kruglyak L, Xu SH, Hu X, Colbert AME, Rosenberg C, Reeve-Daly MP, Rozen S, Hui L, Wu X, Vestergaard C, Wilson KM, Bae JS, Maitra S, Ganiatsas S, Evans CA, DeAngelis MM, Ingalls KA. 1995. An STS-based map of the human genome. Science 270:1945–1954.

Kanegae Y, Lee G, Sato Y, Tanaka M, Nakai M, Sakaki T, Sugano S, Saito I. 1995. Efficient gene activation in mammalian cells by using recombinant adenovirus expressing site-specific Cre recombinase. Nucleic Acids Res 23:3816–3821.

Kanegae Y, Takamori K, Sato Y, Lee G, Nakai M, Saito I. 1996. Efficient gene activation system on mammalian cell chromosomes using recombinant adenovirus producing Cre recombinase. Gene 181:207–212.

Kantor JD, McCormick B, Steeg PS, Zetter BR. 1993. Inhibition of cell motility after nm23 transfection of human and murine tumor cells. Cancer Res 53:1971–1973.

Keim D, Hailat N, Melhem R, Zhu XX, Lascu I, Veron M, Strahler J, Hanash SM. 1992. Proliferation-related expression of p19/nm23 nucleoside diphosphate kinase. J Clin Invest 89:919–924.

Koga H, Araki N, Takeshima H, Nishi T, Hirota T, Kimura Y, Nakao M, Saya H. 1998. Impairment of cell adhesion by expression of the mutant neurofibromatosis type2 (NF2) genes which lack exons in the ERM-homology domain. Oncogene 17:801–810.

Lambeth DO, Mehus JG, Ivey MA, Milavetz BI. 1997. Characterization and cloning of a nucleoside diphosphate kinase targeted to matrix of mitochondria in pigeon. J Biol Chem 272:24604–24611.

Lombardi D, Sacchi A, D'Agostino G, Tibursi G. 1995. The association of the Nm23-M1 protein and beta-tubulin correlates with cell differentiation. Exp Cell Res 217:267–271

MacDonald NJ, De la Rosa A, Benedict MA, Freije JM, Krutsch H, Steeg PS. 1993. A serine phosphorylation of Nm23, and not its nucleoside diphosphate kinase activity, correlates with suppression of tumor metastatic potential. J Biol Chem 268:25780–25789.

Makino K, Kuwahara H, Masuko N, Nishiyama Y, Morisaki T, Sasaki J, Nakao M, Kuwano A, Nakata M, Ushio Y, Saya H. 1997. Cloning and characterization of NE-dlg: a novel human homolog of the *Drosophila* discs large (dlg) tumor suppressor protein interacts with the APC protein. Oncogene 14:2425–2433.

Milon L, Rousseau-Merck MF, Munier A, Erent M, Lascu I, Capeau J, Lacombe ML. 1997. nm23-H4, a new member of the family of human nm23/nucleoside diphosphate kinase genes, localised on chromosome 16p13. Hum Genet 99:550–557.

Minn AJ, Boise LH, Thompson CB. 1996. Expression of Bcl-xL and loss of p53 can cooperate to overcome a cell cycle checkpoint induced by mitotic spindle damage. Genes Dev 10:2621–2631.

Miyake H, Hanada N, Nakamura H, Kagawa S, Fujiwara T, Hara I, Eto H, Gohji K, Arakawa S, Kamidono S, Saya H. 1998. Overexpression of Bcl-2 in bladder cancer cells inhibits apoptosis induced by cisplatin and adenoviral-mediated p53 gene transfer. Oncogene 16:933–943.

Munier A, Feral C, Milon L, Pinon VP, Gyapay G, Capeau J, Guellaen G, Lacombe ML. 1998. A new human nm23 homologue (nm23-H5) specifically expressed in testis germinal cells. FEBS Lett 434:289–294.

Nickerson JA, Wells WW. 1984. The microtubule-associated nucleoside diphosphate kinase. J Biol Chem 259: 11297–11304.

Nosaka K, Kawahara M, Masuda M, Satomi Y, Nishino H. 1998. Association of nucleoside diphosphate kinase nm23-H2 with human telomeres. Biochem Biophys Res Commun 243:342–348.

Ogawa K, Takai H, Ogiwara A, Yokota E, Shimizu T, Inaba K, Mohri H. 1996. Is outer arm dynein intermediate chain 1 multifunctional? Mol Biol Cell 7:1895–1907.

Okabe KJ, Kasukabe T, Honma Y, Hayashi M, Hozumi M. 1988. Purification of a factor inhibiting differentiation from conditioned medium of nondifferentiating mouse myeloid leukemia cells. J Biol Chem 263:10994–10999.

Okabe KJ, Kasukabe T, Hozumi M, Honma Y, Kimura N, Baba H, Urano T, Shiku H. 1995. A new function of Nm23/NDP kinase as a differentiation inhibitory factor, which does not require its kinase activity. FEBS Lett 363:311–315.

Postel EH, Ferrone CA. 1994. Nucleoside diphosphate kinase enzyme activity of NM23-H2/PuF is not required for its DNA binding and in vitro transcriptional functions. J Biol Chem 269:8627–8630.

Postel EH, Berberich SJ, Flint SJ, Ferrone CA. 1993. human c-myc transcriptional factor PuF identified as nm23-H2 nucleoside diphosphate kinase, a candidate suppressor of tumor metastasis. Science 261:478–480.

Radinsky R, Weisberg HZ, Staroselsky AN, Fidler IJ. 1992. Expression level of the nm23 gene in clonal populations of metastatic murine and human neoplasms. Cancer Res 52:5808–5814.

Rosengard AM, Krutzsch HC, Shearn A, Biggs JR, Barker E, Margulies IM, King CR, Liotta LA, Steeg PS. 1989. Reduced Nm23/Awd protein in tumor metastasis and aberrant Drosophila development. Nature 342:177–180.

Saya H, Masuko T, Kokunai T, Yagita H, Ijichi A, Taomoto K, Tamaki N, Matsumoto S, Hashimoto Y. 1986. Detection of human glioma-assoiciated antigen by rat monoclonal antibody raised against syngeneic rat glioma cells. J Neurosurg 65:495–502.

Sekido Y, Ahmadian M, Wistuba II, Latif F, Bader S, Wei MH, Duh FM, Gazdar AF, Lerman MI, Minna JD. 1998. Cloning of a breast cancer homozygous deletion junction narrows the region of search for a 3p21.3 tumor suppressor gene. Oncogene 16:3151–3157.

Stahl JA, Leone A, Rosengard AM, Porter L, King CR, Steeg PS. 1991. Identification of a second human nm23 gene, nm23-H2. Cancer Res 51:445–449.

Steeg PS, Bevilacqua G, Kopper L, Thorgeirsson UP, Talmadge JE, Liotta LA, Sobel ME. 1988. Evidence for a novel gene associated with low tumor metastatic potential. J Natl Cancer Inst 80:200–204.

Taylor SS, McKeon F. 1997. Kinetochore localization of murine Bub1 is required for normal mitotic timing and checkpoint response to spindle damage. Cell 89:727–735.

Troll H, Winckler T, Lascu I, Muller N, Saurin W, Veron M, Mutzel R. 1993. Separate nuclear genes encode cytosolic and mitochondrial nucleoside diphosphate kinase in *Dictyostelium discoideum*. J Biol Chem 268:25469–25475.

Venturelli D, Martinez R, Melotti P, Casella I, Peschle C, Cucco C, Spampinato G, Darzynkiewicz Z, Calabretta B. 1995. Overexpression of DR-nm23, a protein encoded by a member of the nm23 gene family inhibits granulocyte differentiation and induces apoptosis in 32Dc13 myeloid cell. Proc Natl Acad Sci USA 92:7435–7439.

Webb PA, Perisic O, Mendola CE, Backer JM, Williams RL. 1995. The crystal structure of a human nucleoside diphosphate kinase, NM23-H2. J Mol Biol 251:574–587.

Wistuba II, Montellano FD, Milchgrub S, Virmani AK, Behrens C, Chen H, Ahmadian M, Nowak JA, Muller C, Minna JD, Gazdar AF. 1997. Deletions of chromosome 3p are frequent and early events in the pathogenesis of uterine cervical carcinoma. Cancer Res 57:3154–3158.

Wu X, Zhao Y, Honn SE, Tomlinson GE, Minna JD, Hong WK, Spitz MR. 1998. Benzo[a]pyrene diol epoxide-induced 3p21.3 aberrations and genetic predisposition to lung cancer. Cancer Res 58:1605–1608.

Yano M, Kanazawa M, Terada K, Namchai C, Yamaizumi M, Hanson B, Hoogenraad N, Mori M. 1997. Visualization of mitochondrial protein import in cultured mammalian cells with green fluorescent protein and effects of overexpression of the human import receptor Tom20. J Biol Chem 272:8459–8465.